

Proceedings

Scandium Aluminium Nitride-Based Film Bulk Acoustic Resonators [†]

Michael Schneider ^{1,*}, Mario DeMiguel-Ramos ², Andrew J. Flewitt ², Enrique Iborra ³ and Ulrich Schmid ¹

¹ Institute of Sensor and Actuator Systems, TU Wien, Gusshausstrasse 27–29, Vienna, Austria; ulrich.e366.schmid@tuwien.ac.at

² Electrical Engineering Division, Department of Engineering, University of Cambridge, 9 JJ Thomson Avenue, Cambridge CB3 0FA, UK; m.demiguelramos@gmail.com (M.D.-R.); ajf@eng.cam.ac.uk (A.J.F.)

³ GMME-CEMDATIC, ETSI de Telecomunicación, Universidad Politécnica de Madrid, Av. Complutense 30, 28040 Madrid, Spain; enrique.iborra@upm.es

* Correspondence: michael.schneider@tuwien.ac.at; Tel.: +43-1-58801-76636

† Presented at the Eurosensors 2017 Conference, Paris, France, 3–6 September 2017.

Published: 18 August 2017

Abstract: Film bulk acoustic resonators (FBAR) are promising candidates to replace surface acoustic wave devices as filters or delay lines, but also offer exciting opportunities as biological or gas sensors. In this work, solidly mounted FBARs were manufactured by substituting commonly used pure aluminium nitride (AlN) by scandium doped aluminium nitride (ScAlN) thin films as the piezoelectric layer. The ScAlN-based resonators feature a significant improvement of the electromechanical coupling factor from ~3% to ~12% compared to the pure AlN, while the decreased stiffness of ScAlN results in a decrease of the quality factor from ~300 to ~100 due to increased damping losses in the piezoelectric material.

Keywords: film bulk acoustic resonator; FBAR; solidly mounted resonator; SMR; aluminium nitride; scandium aluminium nitride; electromechanical coupling factor; network analyser

1. Introduction

In the last decade, bulk acoustic wave (BAW) devices have almost completely replaced surface acoustic wave (SAW) devices for highly demanding filtering applications such as duplexers in modern electronics [1,2]. In addition, significant research efforts are targeted towards BAW based mass sensors for biological, chemical or physical sensing applications [3–7]. Most commercially available BAW devices are based on aluminium nitride (AlN) thin films due to its high stiffness and CMOS compatibility [1]. The major drawbacks of AlN are the relatively low piezoelectric coefficients ($d_{33,f} = 3.9$ pm/V) and the relatively low intrinsic electromechanical coupling factor ($d_{33,f}^2 \cdot c_{33}^E / \varepsilon_0 \varepsilon_{33} = 6.5\%$ with the stiffness tensor c_{ij}^E and the thin film permittivity tensor $\varepsilon_0 \varepsilon_{ij}$) [8]. In recent years, there has been an ongoing effort to replace AlN by scandium doped AlN (ScAlN) in micro electromechanical systems (MEMS) as well as in SAWs and BAWs for enhanced performance [9–11]. In this work, we demonstrate superior properties of ScAlN-based solidly mounted resonators (SMR) compared to AlN-based devices.

2. Materials and Methods

The devices are fabricated on (100) silicon wafer substrates covered with an acoustic Bragg reflector of 5 alternating layers of silicon dioxide (SiO₂) and molybdenum (Mo), starting with SiO₂. The thickness of the SiO₂ and Mo layers are 521 and 629 nm, respectively, which is optimized for a maximum reflectivity of the longitudinal acoustic wave at 2.5 GHz. The fabrication of the reflector is

discussed in more detail in [12]. The reflector is then consecutively covered by sputter-deposited chromium and iridium thin films with thickness of 15 and 150 nm, respectively. Chromium serves to improve iridium adhesion. Subsequently, aluminium nitride or scandium doped AlN is sputter-deposited on the metallic bottom electrode with a thickness of 1250 nm under nominally unheated substrate conditions. Pure AlN is deposited from a 6" aluminium target with a plasma power of 800 W, a chamber pressure of 2 μbar and in pure nitrogen atmosphere with a constant flow of 50 sccm. ScAlN is deposited from a 4" pre-alloyed ScAl target (27_{at%}:73_{at%}) with a plasma power of 400 W, a chamber pressure of 2.5 μbar and in a mixed argon/nitrogen atmosphere with flow rates of 30 and 20 sccm respectively. The target to substrate distance was fixed at 65 mm in both cases. More details on the deposition of AlN and ScAlN can be found in [11,13]. A 150 nm molybdenum layer is deposited and patterned by wet chemical etching to create the top electrical contacts. The device is contacted in a ground-signal-ground (GSG) configuration with a capacitive coupling of the ground contacts to the iridium layer, which serves as the bottom electrode. This is illustrated in Figure 1. All manufactured devices were characterized by measuring the S_{11} parameter using a signal network analyser (SNA) E5062A from Agilent Technologies.

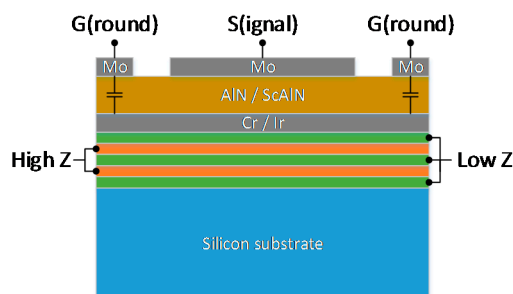


Figure 1. Schematic cross-sectional view on the SMR device investigated in this work.

3. Results and Discussion

Figure 2a shows a comparison between the absolute impedance (Z) spectrum of multiple AlN and ScAlN-based SMR devices. The series resonance frequency f_s is lower for the ScAlN-based device, which can be directly attributed to the ~30% lower stiffness constant c_{33} of ScAlN compared to AlN [14]. This results in a ~17% lower longitudinal acoustic velocity v_3 because $v_3 \propto \sqrt{c_{33}}$. Therefore, there is a similar decrease in the series resonance frequency according to $f_s = v_3/\lambda$ with the wavelength λ being determined by the thickness of the piezoelectric thin film. This decrease of the stiffness constant of ScAlN also results in increased damping losses, which can be seen by the reduced Q-factor of the ScAlN-based devices, as shown in Table 1. The electromechanical coupling factor k_{eff}^2 is calculated according to:

$$k_{eff}^2 = 100 \cdot \left\{ \frac{\pi}{2} \cdot \frac{f_s}{f_p} \right\} / \left\{ \tan \left(\frac{\pi}{2} \cdot \frac{f_s}{f_p} \right) \right\} \quad (1)$$

where f_p is the parallel resonance frequency [1,15]. The ScAlN-based SMR features an increase in k_{eff}^2 by a factor of 4 up to $k_{eff}^2 = 12.18\%$, which is a remarkably high value compared to the AlN-based device with a maximum of $k_{eff}^2 = 3.14\%$. This increase is also clearly visible in the increased separation of f_s and f_p for ScAlN-based SMRs in Figure 2a, as k_{eff}^2 can alternatively (but less accurately) be calculated as $k_{eff}^2 = \{\pi^2(f_p - f_s)\}/4f_p$ and thus $k_{eff}^2 \propto (f_p - f_s)$.

Table 1. SMR device parameters of both ScAlN and AlN-based resonators.

Device	f_s	f_p	Q_s	Q_p	k_{eff}^2
ScAlN, a6	2.123	2.231	101.1	158.1	11.37
ScAlN, a7	2.109	2.225	96.3	178.8	12.18
ScAlN, a9	2.098	2.206	109.2	173.4	11.49
AlN, a1	2.5	2.528	300.6	559.6	2.71
AlN, a6	2.509	2.542	261.6	346	3.14

Figure 2b shows the impact of different resonator surface areas on the performance of ScAlN-based SMRs and the corresponding device parameters are given in Table 2. The shifts in the both the series and parallel resonance frequency can be attributed to inhomogeneity in the film thickness of the ScAlN layer due to the small target size. The baseline increases with the surface area due to the increase in the capacitance of the device.

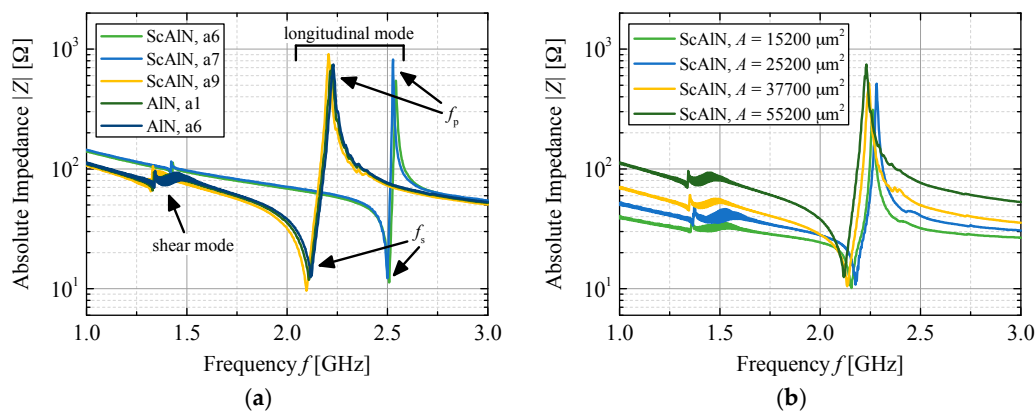


Figure 2. (a) Absolute impedance of SMR devices based on ScAlN and on pure AlN. The sample number ax denotes samples with the same geometry at different positions on the die; (b) Absolute impedance spectrum of SMR devices with varying surface area A .

Table 2. SMR device parameters of ScAlN-based devices with varying resonator area.

Area [μm^2]	f_s	f_p	Q_s	Q_p	k_{eff}^2
15,200	2.123	2.231	101.1	158.1	11.37
25,200	2.141	2.245	87.9	162.5	10.99
37,700	2.183	2.281	128.6	280	10.2
55,200	2.156	2.263	92.4	213.2	11.06

4. Conclusions

In this work, we demonstrated the fabrication of ScAlN-based SMRs and provided a comparison to AlN-based SMRs of identical device geometry. The characteristics of both types of resonators show a significantly increased value of up to $k_{eff}^2 = 12.18\%$ for ScAlN-based devices compared to only $k_{eff}^2 = 3.14\%$ for AlN-based SMRs. This enhanced efficiency comes at the cost of a reduced quality factor and resonance frequency, which can be attributed to the increased damping and reduced stiffness in the softer ScAlN film. Future efforts will focus on how to improve the quality factor while maintaining a high electromechanical coupling.

Acknowledgments: This work has been supported by the ERC within the COST action IC1208, Horizon 2020 research and innovation program under grant agreement No 636820, and by the Ministerio de Economía y Competitividad del Gobierno de España under grant MAT2013-45957-R.

Conflicts of Interest: The authors declare no conflict of interest.

References

1. Ruby, R. Review and Comparison of Bulk Acoustic Wave FBAR, SMR Technology. In Proceedings of the IEEE Ultrasonics Symposium, New York, NY, USA, 28–31 October 2007; pp. 1029–1040.
2. Ruby, R. A Snapshot in Time: The Future in Filters for Cell Phones. *IEEE Microw. Mag.* **2015**, *16*, 46–59, doi:10.1109/MMM.2015.2429513.
3. Cannatà, D.; Benetti, M.; Verona, E.; Varriale, A.; Staiano, M.; Auria, S.D.; Pietrantonio, F.D. Odorant detection via Solidly Mounted Resonator biosensor. In Proceedings of the IEEE International Ultrasonics Symposium, Dresden, Germany, 7–10 October 2012; pp. 1537–1540.
4. Hoffmann, R.; Schreiter, M.; Heitmann, J. The concept of thin film bulk acoustic resonators as selective CO₂ gas sensors. *J. Sens. Sens. Syst.* **2017**, *6*, 87–96, doi:10.5194/jsss-6-87-2017.
5. Chen, Y.C.; Shih, W.C.; Chang, W.T.; Yang, C.H.; Kao, K.S.; Cheng, C.C. Biosensor for human IgE detection using shear-mode FBAR devices. *Nanoscale Res. Lett.* **2015**, *10*, 69, doi:10.1186/s11671-015-0736-3.
6. Chen, D.; Wang, J.; Xu, Y.; Li, D.; Zhang, L.; Li, Z. Highly sensitive detection of organophosphorus pesticides by acetylcholinesterase-coated thin film bulk acoustic resonator mass-loading sensor. *Biosens. Bioelectron.* **2013**, *41*, 163–167, doi:10.1016/j.bios.2012.08.018.
7. DeMiguel-Ramos, M.; Díaz-Durán, B.; Escolano, J.M.; Barba, M.; Mirea, T.; Olivares, J.; Clement, M.; Iborra, E. Gravimetric biosensor based on a 1.3 GHz AlN shear-mode solidly mounted resonator. *Sens. Actuators B Chem.* **2017**, *239*, 1282–1288, doi:10.1016/j.snb.2016.09.079.
8. Trolrier-McKinstry, S. Muralt, P. Thin Film Piezoelectrics for MEMS. *J. Electroceram.* **2004**, *12*, 7–17, doi:10.1023/b:jecr.0000033998.72845.51.
9. Wang, Q.; Lu, Y.; Mishin, S.; Oshmyansky, Y.; Horsley, D.A. Design, Fabrication, and Characterization of Scandium Aluminum Nitride-Based Piezoelectric Micromachined Ultrasonic Transducers. *J. Microelectromech. Syst.* **2017**, *PP*, 1–8, doi:10.1109/JMEMS.2017.2712101.
10. Teshigahara, A.; Hashimoto, K.Y.; Akiyama, M. Scandium aluminum nitride: Highly piezoelectric thin film for RF SAW devices in multi GHz range. In Proceedings of the IEEE International Ultrasonics Symposium, Dresden, Germany, 7–10 October 2012; pp. 1–5.
11. Mayrhofer, P.M.; Rehlehd, C.; Fischeneder, M.; Kucera, M.; Wistrela, E.; Bittner, A.; Schmid, U. ScAlN MEMS Cantilevers for Vibrational Energy Harvesting Purposes. *J. Microelectromech. Syst.* **2017**, *26*, 102–112, doi:10.1109/JMEMS.2016.2614660.
12. DeMiguel-Ramos, M.; Mirea, T.; Olivares, J.; Clement, M.; Sangrador, J.; Iborra, E. Assessment of the shear acoustic velocities in the different materials composing a high frequency solidly mounted resonator. *Ultrasonics* **2015**, *62*, 195–199, doi:10.1016/j.ultras.2015.05.017.
13. Schneider, M.; Bittner, A.; Schmid, U. Improved piezoelectric constants of sputtered aluminium nitride thin films by pre-conditioning of the silicon surface. *J. Phys. D Appl. Phys.* **2015**, *48*, doi:10.1088/0022-3727/48/40/405301.
14. Mayrhofer, P.M.; Euchner, H.; Bittner, A.; Schmid, U. Circular test structure for the determination of piezoelectric constants of Sc_xAl_{1-x}N thin films applying Laser Doppler Vibrometry and FEM simulations. *Sens. Actuators. A Phys.* **2015**, *222*, 301–308, doi:10.1016/j.sna.2014.10.024.
15. Olivares, J.; Wegmann, E.; Clement, M.; Capilla, J.; Iborra, E.; Sangrador, J. Assessment of solidly mounted resonators with wide-band asymmetric acoustic reflectors. In Proceedings of the IEEE International Ultrasonics Symposium, San Diego, CA, USA, 11–14 October 2010; pp. 1677–1680.

